Süleyman Demirel Üniversitesi
Fen Bilimleri Enstitüsü Dergisi
Cilt 29, Sayı 2, 327-334, 2025

Süleyman Demirel University
Journal of Natural and Applied Sciences
Volume 29, Issue 2, 327-334, 2025

DOI: 10.19113/sdufenbed.1667647

Theoretical Insight For The Diels-Alder Reaction Mechanism Between Pyrrole And Acrylonitrile

Aslı ÖZTÜRK KİRAZ*

Pamukkale University, Faculty of Science, Department of Physics, Computational Physics Laboratory, 20030, Denizli, Türkiye

(Alınış / Received: 28.03.2025, Kabul / Accepted: 03.06.2025, Online Yayınlanma / Published Online: 25.08.2025)

Keywords
Reaction mechanism,
Transition state,
Diels-Alder,
Thermal properties

Abstract: Diels Alder reactions are the best method used for the synthesis of various important molecules. In this study, the reaction mechanism between pyrrole and acrylonitrile, which can be an example of these reactions, is explained by DFT. Using the B3LYP method with the 6-31+G(d,p) basis set, chemical hardness, softness, electrophilicity index, electrochemical potential and thermodynamic properties were calculated. When we calculated these properties with solvents such as toluene, the gap between the HOMO and LUMO orbitals of the product formed as a result of the DA reaction was 9.53 eV in the gas phase, while it decreased to 6.49 eV in the toluene solvent environment. In addition, as a result of the calculations; thermodynamic parameters such as enthalpy, entropy and internal energy increased with increasing temperature, but the Gibbs free energy decreased.

Pirol Ve Akrilonitril Arasındaki Diels-Alder Reaksiyon Mekanizmasının Teorik Olarak İncelenmesi

Anahtar Kelimeler
Reaksiyon mekanziması,
Geçiş durumu,
Diels-Alder,
Thermal özellikler

Öz: Diels Alder reaksiyonları çeşitli önemli moleküllerin sentezinde kullanılan en iyi yöntemdir. Bu çalışmada bu reaksiyonlara örnek olabilecek pirol ve akrilonitril arasındaki reaksiyon mekanizması DFT ile açıklanmıştır. 6-31+G(d,p) baz setli B3LYP yöntemi kullanılarak kimyasal sertlik, yumuşaklık, elektrofiliklik indeksi, elektrokimyasal potansiyel ve termodinamik özellikler hesaplanmıştır. Bu özellikleri toluen gibi çözücülerle hesapladığımızda DA reaksiyonu sonucu oluşan ürünün HOMO ve LUMO orbitalleri arasındaki boşluk gaz fazında 9,53 eV iken, toluen çözücü ortamında 6,49 eV'ye düşmüştür. Ayrıca hesaplamalar sonucunda; entalpi, entropi ve iç enerji gibi termodinamik parametreler artan sıcaklıkla artmış, ancak Gibbs serbest enerjisi azalmıştır.

1. Introduction

The Diels–Alder cycloaddition (DA)[1] is a highly effective reaction for forming new carbon-carbon bonds, making constituting a crucial method in the synthesis of various compounds, including pharmaceuticals, macromolecules, and self-healing materials [2-8]. This reaction occurs between a conjugated diene and an alkene, referred to as a dienophile, resulting in a cyclic compound, typically a six-membered ring. While considerable research has been conducted on the DA reaction, its mechanism remains somewhat contentious. In a DA reaction, these two reactants undergo a [4 + 2] cycloaddition mechanism, converting one π bond into two σ bonds [9]. Developed by Otto Diels and Kurt Alder in 1928, this reaction is now regarded as one of the most reliable methodologies in organic chemistry. The DA reaction continues to hold substantial importance as significant today as it was 50 years ago, particularly in synthesizing biologically active natural products [10]. It is prized for its efficiency and precision in controlling stereochemistry, establishing itself as an indispensable tool for organic chemists aiming to streamline the synthesis of complex molecular structures [11-12]. Its extensive applicability in organic synthesis, and its complex mechanistic aspects, position the DA reaction as a vital area for ongoing research and innovative development [13-16]. The reaction may proceed in one or two steps,

*Corresponding author: aslio@pau.edu.tr

depending on the symmetry of the orbitals involved and geometric constraints. The one-step pathway simultaneously forms two carbon-carbon bonds, whereas the two-step mechanism allows for a more gradual formation [17-19].

Pyrrole is a heteroaromatic molecule known for its electron-rich characteristics. It features a five-membered ring that includes one nitrogen atom and four carbon atoms. In contrast, acrylonitrile is a colorless, volatile, and flammable organic compound with a mildly pungent odor. Recent studies have examined the DA reaction involving acrylonitrile and pyrrole [20-22] as shown in Figure 1. Notably, this reaction can be conducted on a microscale without significantly lowering the yields. The application of the In materials engineering, the Diels-Alder reaction is not a novel field of study, it encompasses a broad range of fields, including synthetic chemistry, pharmaceuticals, and biomedical research [23].
The purpose of this study is to use computational techniques to examine the mechanism of reaction between these two compounds. In both the gas phase and the toluene solution, calculations were carried out using density functional theory (DFT). The strong hydrogen-bonding solvent trifluoroethanol has been shown to speed up the Diels-Alder reactions [24], possibly at speeds similar to those of water. DFT is employed to clarify the interactions between the diene and the dienophile [25]. Recognized for its ability to provide accurate results for both organic and inorganic systems, DFT is well-suited for examining the Diels-Alder reaction. However, it is still uncertain whether the anticipated product will result from the reaction, as there is currently no established method to predict the formation of the product.

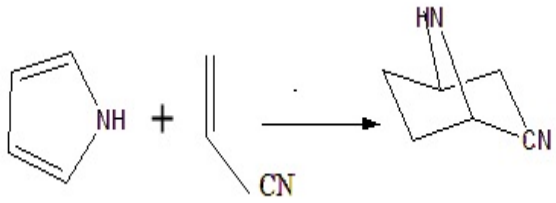

Figure 1. Reaction of pyrrole with acrylonitrile

2. Material and Method

Gaussian 16 [26] was used for the calculations and design of the molecules for this work [27] and GaussView 6.0 was also used for visualization of the structures [28]. Initially, optimization was performed using the 6-31+G (d,p) basis set and DFT with the CAM-B3LYP method [29]. To investigate the effect of solvent on chemical reaction, toluene was employed as a solvent around the bond in calculations utilizing the IEFPCM (Integral Equation Formalism Polarizable Continuum Model) model [30].
Furthermore, chemical hardness (η) and chemical softness from energies of frontier molecular orbitals were calculated by using the following equations [31].

$$\text{Chemical hardness } (\eta) = \frac{E_{LUMO} - E_{HOMO}}{2}$$

$$\text{Chemical softness } S = \frac{1}{2\eta}$$

$$\text{Electrophilicity index } (\mu) = \frac{E_{LUMO} + E_{HOMO}}{2}$$

$$\text{Electronic chemical potential } (\omega) = \frac{\mu^2}{2\eta}$$

3. Results

The optimized geometry of the reactants, product, and transition state are shown in Figure 2, Figure 3, and Figure 4.

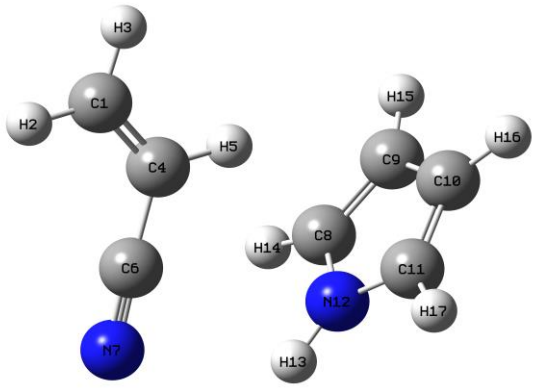

Figure 2. Structure of reactants with numbering and labels.

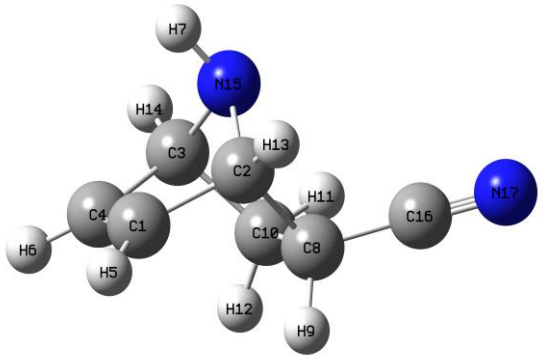

Figure 3. Structure of product with numbering and labels.

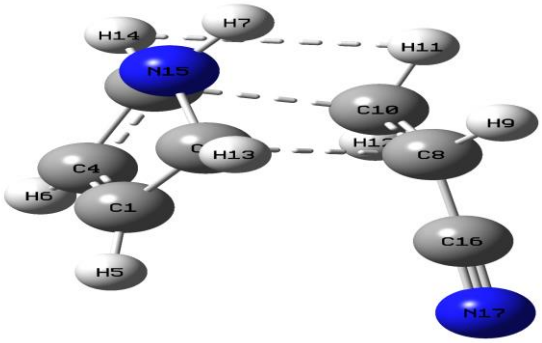

Figure 4. Structure of the transition state with numbering and labels.

3.1. Dipole moment

The dipole moment is a crucial indicator of whether a reaction is proceeding in the correct direction [32]. Specifically, if the dipole moment of the transition state is greater than that of the reactants, it suggests that the reaction pathway is valid, conversely, if it is not, the pathway may not be viable [33]. In the cycloaddition reaction between pyrrole and acrylonitrile, a transition state (TS) is defined as the highest energy unstable intermediate structure that reactants pass through before turning into products during a chemical reaction is generated. The dipole moment of TS measures 5.6 D, which exceeds those of pyrrole (1.9 D) and acrylonitrile (3.9 D). This observation indicates that the transition state is unstable, and the reaction is likely to proceed. Furthermore, a closer examination of the reaction mechanism reveals that the C8 and C11 atoms of pyrrole approach the C1 and C4 atoms of acrylonitrile to form a product as illustrated in Figure 1 [31]. The Gibbs free energy of all structures relative to the reactants is depicted in Figure 5.

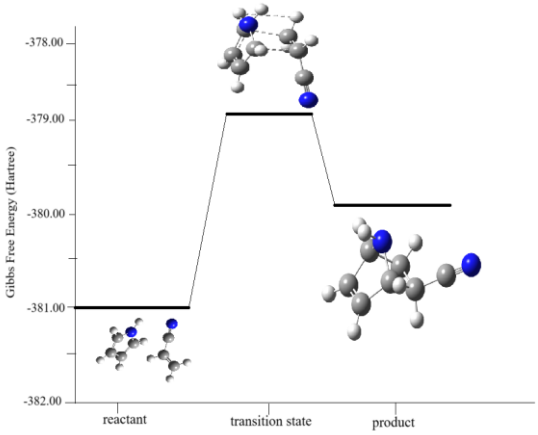

Figure 5. Examining the variations in Gibbs Free Energy among the components of a chemical reaction.

During the reaction, the reaction coordinates change, resulting in the formation of various transition states. When pyrrole and acrylonitrile react, they reach a transition state (TS) that represents the highest energy point in the entire reaction mechanism. If the energy of the products is lower than that of the reactants, a stable product is formed, where the energy is below that of the TS. Ultimately, the reaction yields a product, which possesses an energy lower than that of the reactants.

3.2. Thermodynamics analysis

Thermodynamic properties offer valuable insights into the spontaneity of chemical reactions and the stability of their products [34]. In particular, the reaction between pyrrole and acrylonitrile is exothermic [35]. As shown in Table 1, Table 2, and Table 3, the enthalpy [36], entropy [37], internal energy [37], and heat capacity [37] all rise as the temperature increases from 0 to 300 K, while Gibbs free energy [38] falls. This pattern suggests that raising the temperature is detrimental to this exothermic reaction. The two reactants have in fact reacted, as evidenced by the overall negative energy change and the observed decrease in Gibbs free energy across different states, which points to the formation of an adduct [39]. At 10 K and 300 K, respectively, the reactants' Gibbs free energy is -380.97859 and -381.01736, demonstrating that Gibbs free energy falls with increasing temperature. The formation of a stable product is indicated by the product's Gibbs free energy being higher than the reactants' [40]. The reaction is spontaneous and can happen on its own because the reactants' Gibbs free energy is greater than the products', as shown in Figure 6.

Internal energy, enthalpy, entropy, and heat capacity at constant volume (Cv) are among the other parameters that have been examined. As the graphs in Figure 6 illustrate, these parameters show that all thermodynamic properties increase with temperature while Gibbs free energy decreases. The graphs that accompany the reaction show how temperature affects the reactants, intermediates, and products. Tables 1, 2, 3, 4, and 5 provide specific information on how temperature affects thermodynamic parameters for each step. Gibbs free energy continuously falls with increasing temperature, as shown in Figure 5, even though internal energy, enthalpy, and entropy all rise.

3.3. Electrostatic potential surfaces

The chemical reactivity of molecules can be inferred from their molecular electrostatic potential [40]. The self-consistent field (SCF) method [41] is used to calculate molecular electrostatic potential surfaces (ESP) [42] to describe the process of electron transfer during chemical reactions. The electron density and its quantity are indicated by the ESP in the regions where it is present [41]. It displays the separation between positive charges and electrons. Areas that are green and yellow indicate weak electrophile sites. One can determine which sites of a molecule are most electrophilic and nucleophilic by using a DFT [43] technique. Electrostatic potential increases from red to yellow to green to blue. Different densities are represented by different colors on these maps, which show the regions of electron densities in molecules [44]. Acrylonitrile's carbon atoms C8 and C10 migrate in the direction of pyrrole's carbon atoms C2 and C3 during the reaction. The region surrounding the nitrogen atom in acrylonitrile is recognized as an electron-rich site in the ESP of these two compounds, as shown in Figure 6.

Table 1. Calculated thermodynamic values of reactants by DFT/CAM-B3LYP/6-31+G(d,p)

Tem (K)	C_V (cal/mol-K)	U Hartree)	H (Hartree)	S (cal/mol-K)	G (Hartree)
10	7.016	-380.977	-380.9779	43.044	-380.978
50	15.657	-380.977	-380.9769	64.232	-380.9821
100	18.450	-380.975	-380.9754	77.425	-380.9878
150	21.037	-380.974	-380.9737	86.174	-380.9943
200	24.596	-380.972	-380.9717	93.262	-381.0014
250	28.943	-380.970	-380.9694	99.650	-381.0091
300	33.615	-380.966	-380.9668	105.701	-381.0173

Table 2. Calculated thermodynamic values of the product by DFT/B3LYP/6-311G(d,p)

Tem (K)	C_V (cal/mol-K)	U (Hartree)	H (Hartree)	S (cal/mol-K)	G (Hartree)
10	5.962	-380.660	-380.6602	41.545	-380.6609
50	7.320	-380.659	-380.6597	54.804	-380.6641
100	9.949	-380.659	-380.6589	62.062	-380.6688
150	13.034	-380.658	-380.6578	67.459	-380.6739
200	16.987	-380.657	-380.6564	72.300	-380.6795
250	21.763	-380.655	-380.6547	77.034	-380.6854
300	26.989	-380.653	-380.6526	81.823	-380.6918

Table 3. Calculated thermodynamic values of the transition state of DA reaction by DFT/CAM-B3LYP/6-31+G(d,p)

Tem (K)	C_V (cal/mol-K)	U (Hartree)	H (Hartree)	S (cal/mol-K)	G (Hartree)
10	5.62	-379.920	-379.9202	41.638	-379.9209
50	7.919	-379.919	-379.9197	55.220	-379.9241
100	11.246	-379.919	-379.9187	63.096	-379.9288
150	14.938	-379.918	-379.9175	69.142	-379.9341
200	19.281	-379.916	-379.9160	74.589	-379.9398
250	24.208	-379.914	-379.9141	79.856	-379.9459
300	29.363	-379.912	-379.9118	85.088	-379.9525

3.4. Electronic properties

Frontier molecular orbitals offer essential insights into the reactivity of molecules and reactants [43], as well as their electron-donating and electron-accepting capabilities. As a result, we calculated the HOMO(Highest Occupied Molecular Orbital)-LUMO (Lowest Unoccupied Molecular Orbital) energy levels and energy gaps for all relevant structures. When kinetic stability and energy gaps are high, the reaction tends to be less reactive, conversely, lower values indicate a more reactive nature [45]. Our findings presented in Table 4 indicate that the HOMO-LUMO energy gap for the transition state (TS) is 3.07 eV, which is notably lower than the gaps observed for the reactants and products. This suggests that the transition state is highly reactive and unstable. If the HOMO of acrylonitrile interacts with the LUMO of pyrrole, the reaction is classified as inverse electron demand [46]. On the other hand, if the HOMO of pyrrole interacts with the LUMO of acrylonitrile, the reaction is considered normal electron demand. The energy values derived from frontier molecular orbitals (FMOs) are instrumental in determining the type of reaction taking place. The energy gap between the HOMO of acrylonitrile and the LUMO of pyrrole was found to be 11.33 eV. In a similar calculation, the gap between the LUMO of acrylonitrile and the HOMO of pyrrole yielded a value of 7.31 eV. The difference in energy gap between the HOMO of pyrrole and the LUMO of acrylonitrile is comparatively smaller than the others, confirming that this reaction is of normal electron demand.

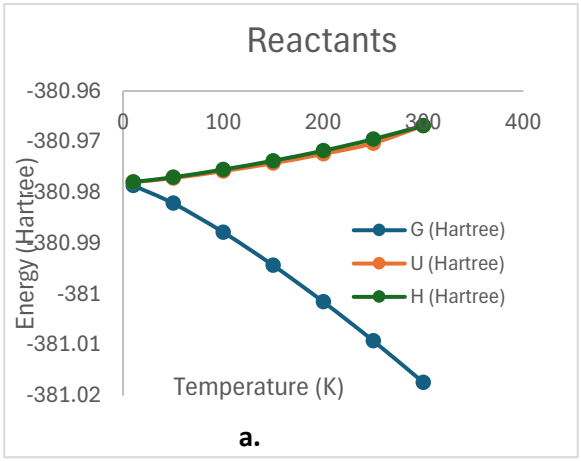

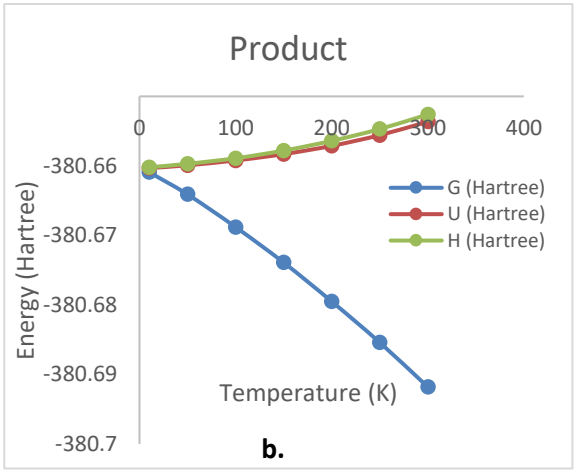

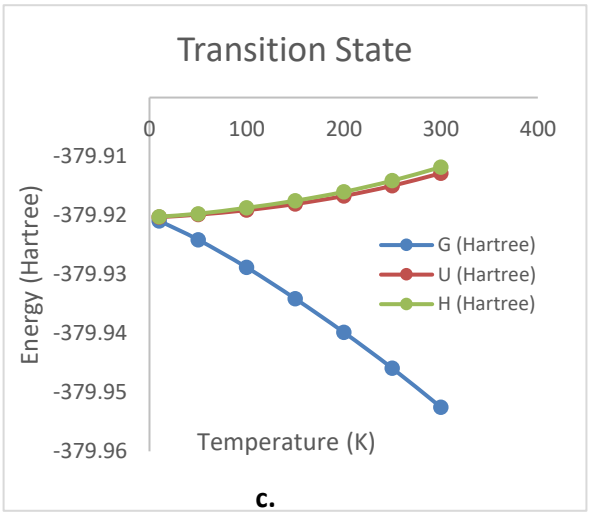

Figure 6. Graph **a.** represent the effect of temperature on reactants, **b.** represent product,
c. represent transition state.

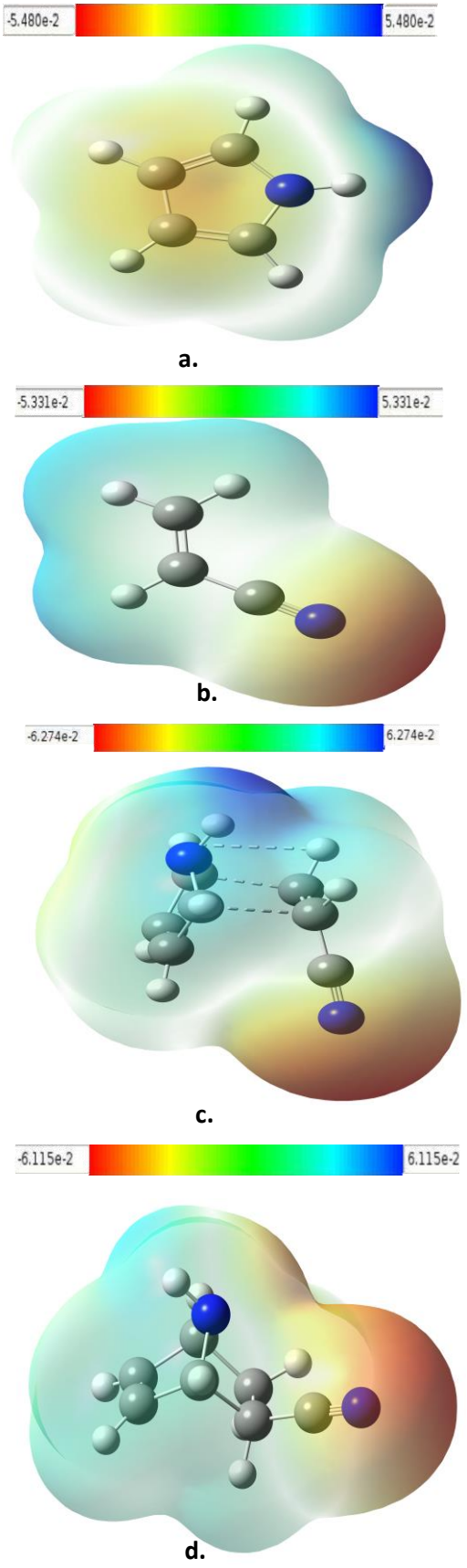

Figure 7. ESP of **a.** pyrrole **b.** acrylonitrile **c.** transition state of the DA reaction **d.** product.

Table 4. HOMO-LUMO energy gap in gas phase calculated by method DFT/CAM-B3LYP/6-31+G(d,p)

Parameters	acrylonitrile		pyrrole		reactants		product		ts	
	gas	toluen	gas	toluen	gas	toluen	gas	toluen	gas	toluen
E_{HOMO} (eV)	-9.46	-9.58	-7.39	-7.45	-6.00	-5.56	-8.22	-8.07	-5.28	-5.50
E_{LUMO} (eV)	-0.08	-1.69	1.87	-2.37	-1.70	-1.56	1.31	-1.587	-2.21	-1.12
$\Delta E = E_{LUMO} - E_{HOMO}$ (eV)	9.38	7.89	9.26	5.08	4.30	3.99	9.53	6.49	3.07	4.38
I (ionization potential) (eV)	9.46	9.58	7.39	7.45	6.00	5.56	8.22	8.07	5.28	5.50
A (electron affinity) (eV)	0.08	1.69	-1.87	2.37	1.70	1.56	-1.31	1.58	2.21	1.12
χ (electronegativity) (eV)	4.77	5.64	2.75	4.91	3.85	3.56	3.46	4.83	3.74	3.31
η (global hardness) (eV)	4.69	3.94	4.63	2.54	2.15	1.99	4.77	3.24	1.54	2.19
S (global softness) (eV^{-1})	0.21	0.25	0.21	0.39	0.46	0.50	0.21	0.31	0.65	0.46
μ (electronic chemical potential) (eV)	-4.77	-5.64	-2.75	-4.91	-3.85	-3.56	-3.46	-4.83	-3.74	-3.31
ω (global electrophilicity index) (eV)	2.42	4.03	0.82	4.74	3.44	3.18	1.25	3.59	4.56	2.50

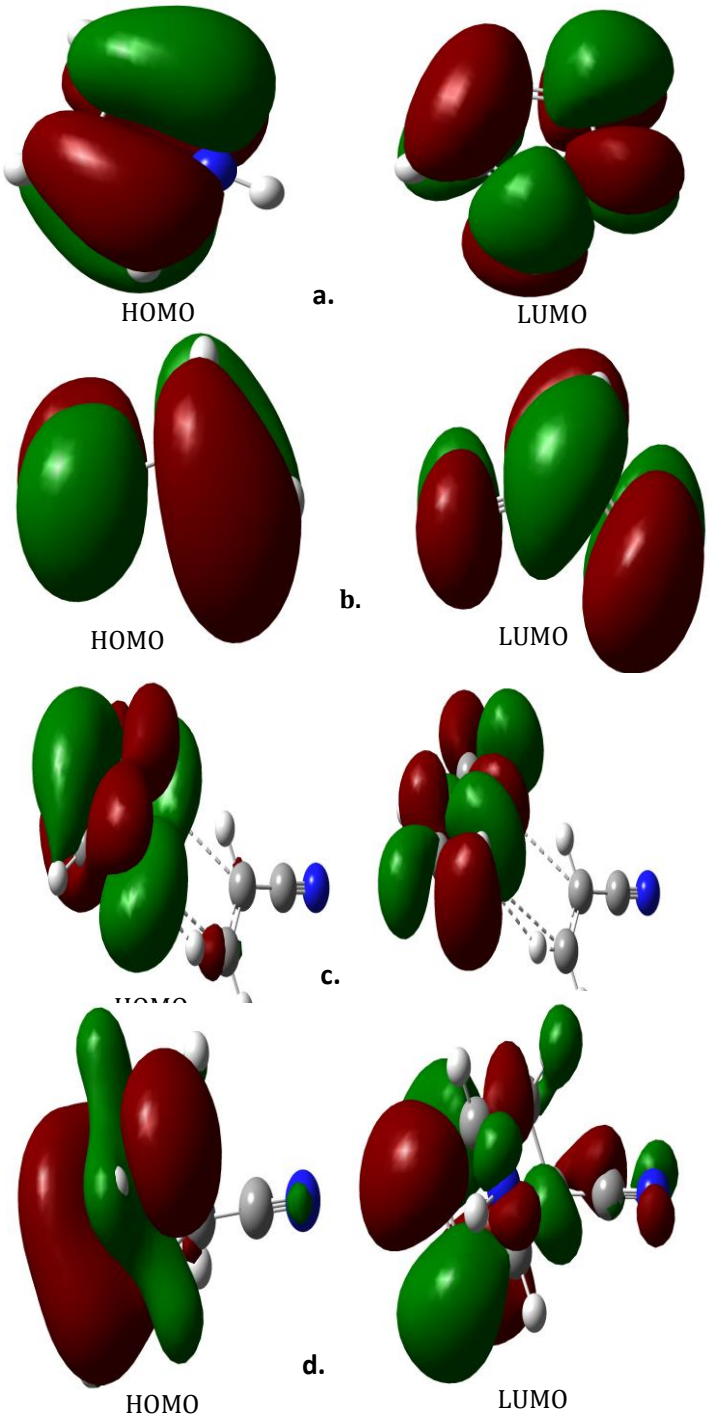

Figure 8. HOMO-LUMO of the **a.** pyrrole **b.** acrylonitrile **c.** transition state **d.** product

It is also observed that the energy gaps for the transition states are consistently lower than those of the reactants and products [47]. The electrophilicity index serves as a measure of a molecule's ability to accept electrons. In this case, because the electrophilicity index value of acrylonitrile exceeds that of pyrrole, acrylonitrile functions as the electrophile. The impact of the solvent on the rate of reaction is investigated using Density Functional Theory (DFT) alongside the Integral Equation Formalism Polarizable Continuum Model (IEFPCM). Our results demonstrate that using toluene as a solvent significantly lowers the activation energy barrier, suggesting an enhanced reaction rate compared to other solvents. This insight is important for optimizing conditions in chemical reactions. The configurations of the HOMO-LUMO orbitals of the reactants, product, and transition state are presented in Figure 8.

4. Discussion and Conclusion

This study shows that for temperature changes ranging from 0 to 300 K, the following thermodynamic quantities significantly increase: enthalpy, internal energy, and heat capacity. However, over this temperature range, Gibbs free energy decreases. This overall increase in these quantities and the concomitant decrease in Gibbs free energy imply that raising the temperature is detrimental to the forward reaction of this exothermic reaction, influencing overall feasibility and efficiency. The reaction products between pyrrole and acrylonitrile have stable structures, which can be inferred from the enormous gap between HOMO and LUMO energies of the resultant products. In addition, these products possess thermodynamic stability. A stable product is formed when the Gibbs free energy of the product is lower than that of the reactants. The toluene solvent exerts a major influence on the reaction rate. Our findings demonstrate that toluene effectively reduces the activation energy barrier compared to other solvents, leading to a markedly increased reaction rate. This understanding is vital for optimizing the milieu of chemical reactions. Such computations are a useful guide for real-world research undertakings.

Acknowledgments

The author would like to thank the TUBITAK/ULAKBIM clusters for their assistance in performing some computations and Pamukkale University, Grand ID: 2018FEBE002 and Dr. Aykut Demirçalı for his support.

Declaration of Ethical Code

In this study, we undertake that all the rules required to be followed within the scope of the "Higher Education Institutions Scientific Research and Publication Ethics Directive" are complied with, and that none of the actions stated under the heading "Actions Against Scientific Research and Publication Ethics" are not carried out.

References

[1] Diels, O., Alder, K. 1928. Synthesen in Der Hydroaromatischen Reihe. Leibigs Ann. Chem. 460, 98–122.

[2] Tasdelen, M. A. 2011. Diels–Alder "click" Reactions: Recent Applications in Polymer and Material Science. Polym. Chem. 2, 2133–2145.

[3] Heravi, M. M., Ahmadi, T., Ghavidel, M., Heidari, B., Hamidi, H. 2015. Recent Applications of the Hetero Diels–Alder Reaction in the Total Synthesis of Natural Products. RSC Adv. 5, 101999 – 102075.

[4] Nicolaou, K. C., Snyder, S. A., Montagnon, T., Vassilikogiannakis, G. 2002. The Diels - Alder Reaction in Total Synthesis. Chem., Int. Ed. 41, 1668.

[5] Kappe, C. O., Murphree, S. S., Padwa, A. 1997. Synthetic Applications of Furan Diels-Alder Chemistry. Tetrahedron 53, 14179–14233.

[6] Funel, J.-A., Abele, S. 2013. Industrial Applications of the Diels-Alder Reaction. Angew. Chem., Int. Ed. 52, 3822–3863.

[7] Peterson, A. M., Jensen, R. E., Palmese, G. R. 2010. Room-Temperature Healing of a Thermosetting Polymer Using the Diels-Alder Reaction. ACS Appl. Mater. Interfaces, 2, 1141–1149.

[8] Zeng, C., Seino, H., Ren, J., Hatanaka, K., Yoshie, N. 2013. Bio-Based Furan Polymers with Self-Healing Ability. Macromolecules, 46, 1794–1802.

[9] U. Rehman, A. Mansha, M. Zahid, S. Asim, A.F. Zahoor, Z.A. Rehan, 2022. Quantum mechanical modeling unveils the effect of substitutions on the activation barriers of the Diels-Alder reactions of an antiviral compound 7H-benzo [a] phenalene, Struct. Chem. 1–14.

[10] B.S. Bodnar, M.J. Miller, 2011. The nitrosocarbonyl hetero-Diels–Alder reaction as a useful tool for organic syntheses, Angew. Chem. Int. Ed. 50, 5630–5647.

[11] D. McLeod, M. K. Thogersen, N. I. Jessen, K. A. Jorgensen, C. S. Jamieson, X.-S. Xue, K. Houk, F. Liu and R. Hoffmann. 2019. Accounts of Chemical Research 52, 3488.

[12] J. S. Barber, M. M. Yamano, M. Ramirez, E. R. Darzi, R. R. Knapp, F. Liu, K. Houk, and N. K. Garg, 2018. Nature Chemistry 10, 953.

[13] A. N. S. Chauhan, G. Mali, and R. D. Erande, 2022. Asian Journal of Organic Chemistry 11, e202100793.

[14] M.-M. Xu, L. Yang, K. Tan, X. Chen, Q.-T. Lu, K. Houk, and Q. Cai, 2021. Nature Catalysis 4, 892.

[15] Y. S. Zholdassov, L. Yuan, S. R. Garcia, R. W. Kwok, A. Boscoboinik, D. J. Valles, M. Marianski, A. Martini, R. W. Carpick, and A. B. 2023. Braunschweig, Science 380, 1053.

[16] S. Chen, P. Yu, and K. Houk, 2018. Journal of the American Chemical Society 140, 18124.

[17] Houk, K. N., Gonzalez, J., Li, Y. 1995. Pericyclic Reaction Transition States: Passions and Punctilios, 1935–1995. Acc. Chem. Res. 28, 81–90.

[18] Houk, K. N., Li, Y., Evanseck, J. D. 1992. Transition Structures of Hydrocarbon Pericyclic Reactions. Angew. Chem., Int. Ed. Engl. 31, 682–708.

[19] Domingo, L. R., José Aurell, M., Pérez, P., Contreras, R. 2003. Origin of the Synchronicity on the Transition Structures of Polar Diels-AlderReactions. Are These Reactions [4 + 2] Processes? J. Org. Chem., 68, 3884–3890.

[20] Xujian Chen, Chengcheng Wei, Min Xie**,** Yongjun Hu, 2023. Single-Photon Ionization Induced New Covalent Bond Formation in Acrylonitrile(AN)–Pyrrole(Py) Clusters. J. Phys. Chem. A, 127, 40, 8272–8279.

[21] Cetiner, S., Kalaoglu, F., Karakas, H. et al. 2011. Characterization of conductive poly(acrylonitrile-*co*-vinylacetate) composites: Matrix polymerization of pyrrole derivatives. Fibers Polym 12, 151–158.

[22] El-Aassar, M.R., Shibraen, M.H.M.A., Abdel-Fattah, Y.R. et al. Functionalization of Electrospun Poly(Acrylonitrile-co-Styrene/Pyrrole) Copolymer Nanofibers for Using as a High-performance Carrier for Laccase Immobilization. Fibers Polym 20, 2268–2279.

[23] Gandini, A., Carvalho, A.J.F., Trovatti, E., Kramer, R.K. and Lacerda, T.M. 2018. Eur. J. Lipid Sci. Technol., Macromolecular materials based on the application of the Diels–Alder reaction to natural polymers and plant oils, 120, 1700091.

[24] Dutt, G., Ghanty, T. 2003. Rotational dynamics of nondipolar probes in ethanols: How does the strength of the solute-solvent hydrogen bond impede molecular rotation? J. Chem. Phys. 119, 4768–4774.

[25] Ali, M., Mansha A., Asim, S., Zahid, M., Usman, Ali, M. N. 2018. DFT study for the spectroscopic and structural analysis of p-dimethylamino azobenzene, J. Spectrosc. 2018, 9365153, 15 pages.

[26] Frisch, M.J., Trucks, G.W., Schlegel, H.B., Scuseria, G.E., Robb, M.A., Cheeseman, J.R.; Scalmani, G.; Barone, V.; Petersson, G.A.; Nakatsuji, H.; Li, X.; Caricato, M.; Marenich, A.V.; Bloino, J., Janesko, B.G., Gomperts, R., Mennucci, B., Hratchian, H.P., Ortiz, J.V., Izmaylov, A.F., Sonnenberg, J.L., Williams-Young, D., Ding, F., Lipparini, F., Egidi, F., Goings, J., Peng, B., Petrone, A., Henderson, T., Ranasinghe, D., Zakrzewski, V.G., Gao, J., Rega, N., Zheng, G., Liang, W., Hada, M., Ehara, M., Toyota, K., Fukuda, R., Hasegawa, J., Ishida, M., Nakajima, T., Honda, Y., Kitao, O., Nakai, H., Vreven, T., Throssell, K., Montgomery Jr., J.A., Peralta, J.E., Ogliaro, F., Bearpark, M.J., Heyd, J.J., Brothers, E.N., Kudin, K.N., Staroverov, V.N., Keith, T.A., Kobayashi, R., Normand, J., Raghavachari, K., Rendell, A.P., Burant, J.C., Iyengar, S.S., Tomasi, J., Cossi, M., Millam, J.M., Klene, M., Adamo, C., Cammi, R., Ochterski, J.W., Martin, R.L., Morokuma, K., Farkas, O., Foresman, J.B., Fox, D.J. 2016. Gaussian 16, Revision B.01, Gaussian, Inc., Wallingford CT.

[27] C. Barros, P. De Oliveira, F. Jorge, A. Canal Neto, M. Campos, 2010. Gaussian basis set of double zeta quality for atoms Rb through Xe: application in non-relativistic and relativistic calculations of atomic and molecular properties, Mol. Phys. 108, 1965–1972.

[28] Dennington, R. Keith, T., Millam, J. GaussView, Version 6. Semichem Inc., Shawnee Mission, KS, 2016.

[29] Jahantigh, F., Ghorashi, S.B., Belverdi, A.R. 2018. A first principle study of benzimidazobenzophenanthrolin and tetraphenyldibenzoperiflanthene to design and construct novel organic solar cells, Phys. B Condens. Matter 542, 32–36.

[30] Zheng, S., Geva, E., Dunietz, B.D. 2013. Solvated charge transfer states of functionalized anthracene and tetracyanoethylene dimers: a computational study based on a range separated hybrid functional and charge constrained self-consistent field with switching Gaussian polarized continuum models, J. Chem. Theory Comput. 9, 1125–1131.

[31] Hussain, R., Saeed, M., Mehboob, M.Y., Khan, S.U., Khan, M.U., Adnan, M., Ahmed, Iqbal, M. J., Ayub, K.J.R. 2020. Density functional theory study of palladium cluster adsorption on a graphene support, 10, 20595-20607.

[32] B. Champagne, E.A. Perp`ete, D. Jacquemin, S.J. Van Gisbergen, E.-J. Baerends, C. Soubra-Ghaoui, K.A. Robins, B. Kirtman. 2000. Assessment of conventional density functional schemes for computing the dipole moment and (hyper) polarizabilities of push–pull π-conjugated systems, Chem. A Eur. J. 104 4755–4763.

[33] Best, R.B., Hummer, G. 2005. Reaction coordinates and rates from transition paths, Proceedings of the National Academy of Sciences, 102, 6732-6737.

[34] Ren, S.-J., Wang, C.-P., Xiao, Y., Deng, J. Tian, Y., Song, J-J., Cheng, X.-J., Sun, G.-F. 2020. Thermal properties of coal during low temperature oxidation using a grey correlation method, Fuel 260, 116287.

[35] DeBoef, B.L. 2003. Novel rhodium catalyzed [4+ 2] and [4+ 2+ 2] cyclization reactions: New methods for the synthesis of six and eight-membered rings, Washington University in St, Louis.

[36] Torres, F.E., Kuhn, P., Bruyker, Bell, D. De A.G., Wolkin, M.V., Peeters, E. Williamson, J.R., Anderson, G.B., Schmitz, G.P., Recht, M.I. 2004. Enthalpy arrays, Proceedings of the National Academy of Sciences, 101, 9517-9522.

[37] Bein, B. 2006. Entropy, Best Practice & Research Clinical Anaesthesiology, 20, 101-109.

[38] Jia, C.-S., Zhang, L.-H., Peng, X.-L., Luo, J.-X. Y.-L. Zhao, J.-Y. Liu, J.-J. Guo, L.- D. Tang, 2019. Prediction of entropy and Gibbs free energy for nitrogen, Chem. Eng. Sci. 202, 70–74.

[39] Zuo, R. Zhang, H., Wang, B.-L. Meng, S.-C. Chen, P., Zhang, R. 2016. Quantum chemistry study on the adduct reaction paths as functions of temperature in GaN/AlN MOVPE growth, ECS J. Solid State Sci. Technol. 5, P667.

[40] Chakraborty, A., Saha, B.B. Ng, K.C., Koyama, S. Srinivasan, K.J.L. 2009. Theoretical insight of physical adsorption for a single-component adsorbent+ adsorbate system: I. Thermodynamic property surfaces, 25, 2204-2211.

[41] Bayoumy, A.M., Ibrahim, M. Omar. A. 2020 Mapping molecular electrostatic potential (MESP) for fulleropyrrolidine and its derivatives, Opt. Quant. Electron. 52, 1–13.

[42] Prabavathi, N., Nilufer, A., Krishnakumar, B. 2013. Spectroscopy, Vibrational spectroscopic (FT-IR and FT-Raman) studies, natural bond orbital analysis and molecular electrostatic potential surface of Isoxanthopterin, 114 101-113.

[43] Obot, I., Macdonald, D. Gasem, Z. 2015. Density functional theory (DFT) as a powerful tool for designing new organic corrosion inhibitors. Part 1: an overview, Corros. Sci. 99, 1–30.

[44] Akinpelu, O.I., Lawal, M.M., Kumalo, H.M. Mhlongo, N.N.J.J.o.B.S.m2022. Dynamics, Computational studies of the properties and activities of selected trisubstituted benzimidazoles as potential antitubercular drugs inhibiting MTB-FtsZ polymerization, 40 1558-1570.

[45] H. Zhang, H. Zhao, X. Wang, Y. Shang, B. Han, Z.J.J.o.m.m. Li, 2014. Theoretical study on the mechanisms of polyethylene electrical breakdown strength increment by the addition of voltage stabilizers, 20, 1-11.

[46] Rohling, R.Y., Tranca, I.C. E.J. Hensen, E.A.J.A.c. Pidko, 2018. Mechanistic Insight into the [4+ 2] Diels-Alder Cycloaddition over First, Row d-Block Cation-Exchanged Faujasites 9, 376–391.

[47] Bendikov, M. Wudl, F. D.F.J.C.r. Perepichka, 2004. Tetrathiafulvalenes, oligoacenenes, and their buckminsterfullerene derivatives: The brick and mortar of organic electronics, 104. 4891-4946.